BWROG-TP-14-001
Revision 0
January 2014

Containment Accident Pressure Committee (344)

Task 1 - CFD Report and Combined NPSHr Uncertainty for Browns Ferry/ Peach Bottom CVIC RHR Pumps

Author:	Dan Baun (Sulzer Pump)
Project Manager:	Kenneth Welch (GEH)
Committee Chairman:	John Freeman (Exelon)

INFORMATION NOTICE

BWROG Utility Members	
CENG – Nine Mile Point	Chubu Electric Power Company
DTE – Fermi	Chugoku Electric Power Company
Energy Northwest – Columbia	Comisión Federal de Electricidad
Entergy – FitzPatrick	Hokuriku Electric Power Company
Entergy – Pilgrim	Iberdrola Generacion, S.A.
Entergy – River Bend/Grand Gulf	Japan Atomic Power Company
	J-Power (Electric Power Development Co.)
Exelon (Clinton)	Kernkraftwerk Leibstadt
Exelon (D/QC/L)	South Texas Project
Exelon (Oyster Creek)	Taiwan Power Company
Exelon (PB/Limerick)	Tohoku Electric Power Company
FirstEnergy – Perry	Tokyo Electric Power Company
NPPD – Cooper	
NextEra – Duane Arnold	
PPL – Susquehanna	
PSEG – Hope Creek	
Duke Energy – Brunswick	
SNC – Hatch	
TVA – Browns Ferry	
Xcel – Monticello	

Executive Summary

This BWROG Technical Product provides a summary of the results of Computational Fluid Dynamics (CFD) studies to model uncertainties in $NPSH_R$ for the CVIC model pump used in the Browns Ferry and Peach Bottom RHR systems, an analysis of the limitations of state-of-the-art CFD codes in predicting pump $NPSH_R$, alternative methods for evaluating the individual $NPSH_R$ uncertainty terms, and a method for combining the individual uncertainty terms to determine an overall pump $NPSH_R$ uncertainty.

Implementation Recommendations

This product is intended for use to address (in part) issues raised in the NRC Guidance Document for the Use of Containment Accident Pressure in Reactor Safety Analysis (ADAMS Accession No. ML102110167). Implementation will be part of the BWROG guidelines on the use of Containment Accident Pressure credit for ECCS pump NPSH analyses.

Benefits to Site

This product provides a technical response to the NRC questions about how utilities account for the uncertainties in pump $NPSH_R$ when evaluating ECCS pump performance in accident conditions.

SULZER

QUALITY LEVEL

- ☐ Direct
- ☐ Indirect

SULZER PUMPS (US) INC. DOCUMENT

DOC. NO: E12.5.1991
ORDER NO: 100072780

TITLE: Task 1 - CFD Report and Combined NPSHr Uncertainty for Browns Ferry/ Peach Bottom CVIC RHR Pumps
Sulzer Pumps (US) Inc.
Browns Ferry/Peach Bottom – RHR Pumps

ASME CODE SECTION

CLASS NO.

CODE EDITION (YEAR)

CUSTOMER GE-HITACHI Nuclear Energy Americas LLC

PROJECT Browns Ferry/Peach Bottom Nuclear Power Stations

CUSTOMER P.O. NO. 437054820

CONTRACT NUMBER

SPECIFICATION NO.

ITEM / TAG NUMBER

CUSTOMER APPROVAL NUMBER:

SPACE FOR CUSTOMER APPROVAL STAMP (when applicable/available)

CUSTOMER APPROVAL REQUIREMENT

☐ Yes ☐ No ☑ Information Only

CERTIFIED AS A VALID SULZER PUMPS (US) INC. DOCUMENT

☐ For Outside Vendor

☒ For Manufacture at Sulzer Pumps (US) Inc.

☐ Risk Release Inspection Report # ______

☐ Other (specify) ______

APPROVALS (SIGNATURE)		Date
Engineering	[signature]	11/26/13

CERTIFICATION (when applicable)

This Document is certified to be in compliance with THE APPLICABLE PURCHASE ORDER, SPECIFICATIONS, PROCEDURES, AND ADDITIONAL REQUIREMENTS LISTED IN THE APPENDICES.

Professional Engineer

State Registration No.

Date ______

Originating Dept: Advance Engineering

By: Daniel Baun

Title: Adv. Eng. Manager, Power and Water Segments

Date: 11/26/2013

APPLICABLE S.O. NUMBERS:
270671/82
270683/90

DOCUMENT IDENTIFICATION	Rev.
E12.5.1991	0

TABLE OF CONTENTS

1.0 CFD ANALYSIS

A computational fluid dynamics (CFD) analysis of the Browns Ferry and Peach Bottom (henceforth referred to as Browns Ferry) 18x24x28 CVIC model pump was undertaken with the objective of quantifying the effect of various pump and system parameters on the pump's required net positive suction head (NPSHr) characteristic. In part, the analysis was intended to establish the efficacy of CFD in quantifying the individual influence as well as the combined influences of the following variables on the pump NPSHr: 1) plant piping geometry 2) fluid temperature 3) dissolved gas and, 4) wear ring clearance.

The Browns Ferry and Peach Bottom Residual Heat Removal (RHR) system pumps are 18x24x28 CVIC pumps. The Sulzer CVIC pump is a vertically arranged, overhung, single stage, single suction centrifugal pump configured with a double volute and in-line suction and discharge nozzles. The pump uses a four vane impeller design with an inlet vane tip diameter of [[ ]] and a maximum impeller outer diameter of [[ ]]. The impeller has both a front and rear wear ring as well as impeller thrust balancing holes. The overhung impeller is mounted to a short stub shaft that is supported in a product lubricated bearing before being rigidly coupled to the shaft of the drive motor. The pump industry standard practice for characterizing specific speed and suction specific speed is to use a pump's full diameter discharge and suction characteristics, respectively. The Browns Ferry RHR CVIC full diameter pump specific speed ($Ns = RPM*Q^{0.5}/H^{0.75}$) is [[ ]] and the suction specific speed ($Nss = RPM*Q^{0.5}/NPSHr^{0.75}$) is [[ ]].

Figures 1, 2, and 3 show different views of the 3D geometric model used for the baseline CFD simulations. For CFD modeling purposes, approximately 1 meter (3.28 ft) of straight pipe was added to the pump inlet and discharge nozzles as well as a converging section on the pump discharge exit as shown in Figure 1. These inlet and exit pipe modeling additions were necessary to prevent recirculating flows from crossing the inlet and exit CFD computational domain boundary planes during the solution process. An overview of the solver settings and the mesh characteristics is provided in Tables 1 and 2, respectively. The Figure 4 pump characteristic curves are based on Curve 1, RHR Average Performance, from Sulzer Report, E12.5.1296 Revision 3, December 28, 2010, normalized to full pump impeller diameter, 27.5 inches.

1.1 CFD Model and Simulation Set-Up

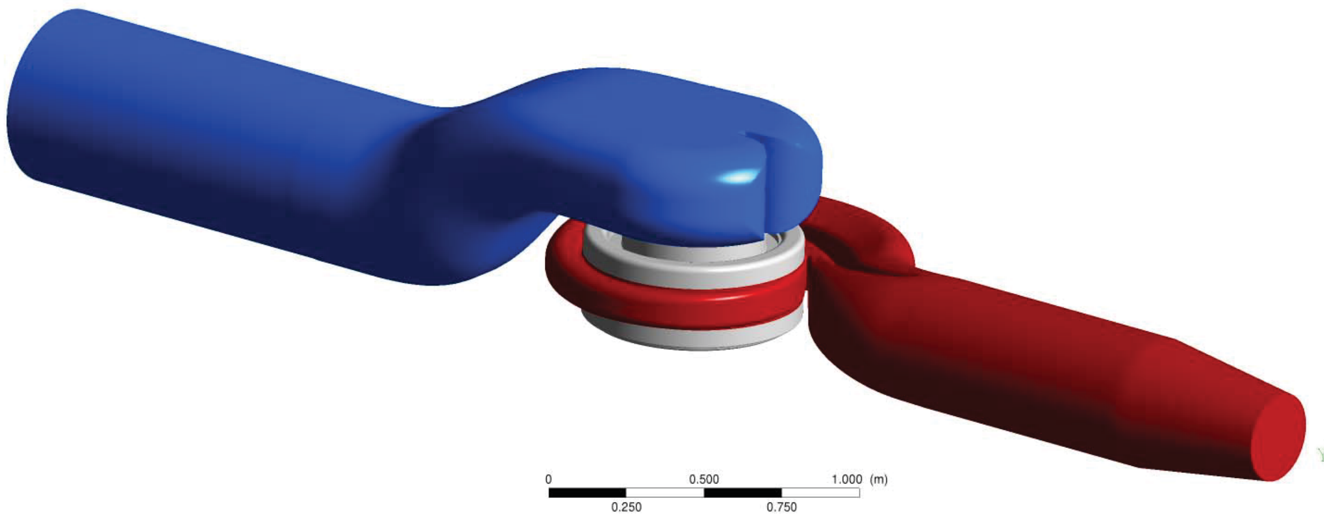

Figure 1: Browns Ferry CVIC CFD Model - Isometric View

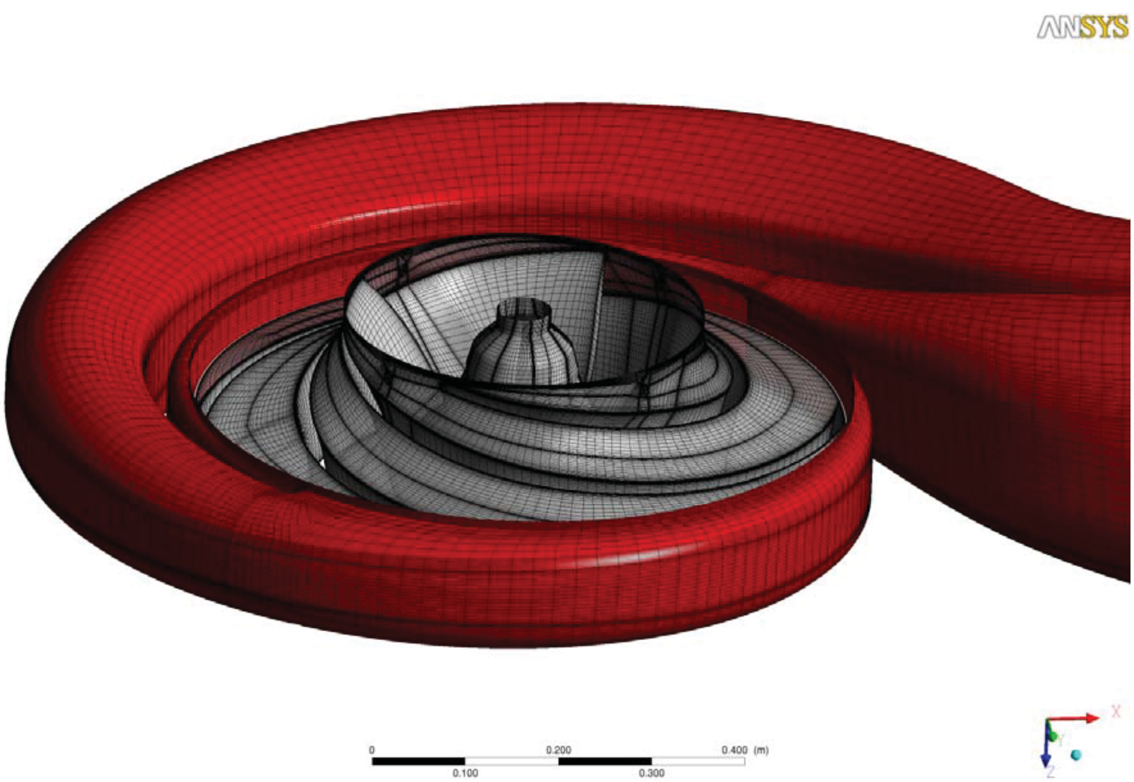

Figure 2: Browns Ferry CVIC CFD Model - Side View

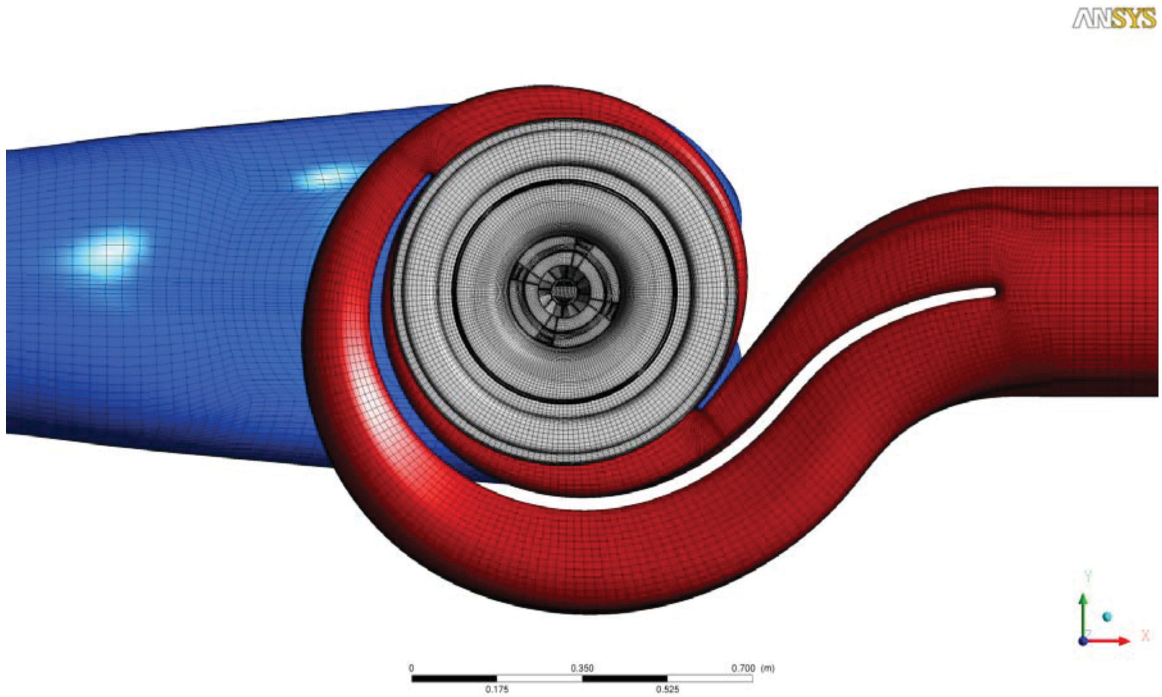

Figure 3: Browns Ferry CVIC CFD Model - Plan View

The CFD work for this project was performed under contract by Sulzer Innotec. The CFD code employed on the project was ANSYS CFX 13.0, a well-documented and validated commercial RANS (Reynolds Averaged Navier Stokes) based finite volume general purpose CFD solver. The key CFD solver set-up and configuration metrics are given in Table 1. A structured multi-block CFD mesh, consisting of approximately [[ ]] elements was used for the full pump model. The mesh breakdown statistics are summarized in Table 2.

Item	Setting
Code Type	[[
Turbulence	
Advection Scheme	
Cavitation	
Inlet B.C.	
Outlet B.C.	
Simulation Type	
MFR Setting	]]

Table 1: Browns Ferry CVIC CFD Model Boundary Conditions and Solver Settings

Domain	Element Count
Suction Casing	[[
Impeller	
Side Rooms / Seals	
Volute	]]

Table 2: Browns Ferry CVIC CFD Model Grid/Mesh Statistics

1.2 Discussion of CFD Results

A baseline set of CFD simulations was run at flow rates (Q) of [[ ]] to compare with the tested pump curve. These flows correspond to normalized pump flows (Q*) of [[ ]], respectively. The normalized flow (Q*) is defined as the flow rate (Q) divided by the best efficiency flow (Q_{BEP}),

$Q^* = Q/Q_{BEP}$. The baseline CFD model included the complete pump geometry with a straight inlet pipe (blue pipe segment on left side of Figure 1) and was run as a steady-state simulation with Frozen Rotor grid interfaces applied at both the impeller inlet and exit.

[[

]]

Figure 4: 18x24x28 CVIC Full Diameter Pump Performance Overlaid with CFD Simulation Results from Baseline Model @ [[ ]]

The baseline CFD head, efficiency, and 3% pump head breakdown (NPSH3) simulation results showed good agreement with the manufacturer's averaged test bed measured performance as shown in Figure 4. At BEP of [[ ]], the CFD predicted pump head was [[ ]] higher than the tested head, the CFD predicted efficiency was approximately [[ ]] lower than the tested efficiency, and the CFD predicted NPSH3 was approximately [[ ]] higher than the tested NPSH3. While the comparison between the simulated NPSH3 and the test NPSH3 characteristics are good at the BEP flow, the deviations between the two curves increase to approximately [[ ]] and [[ ]].

2.0 CFD Results and Analysis of Parameter Effects on NPSHr

2.1 Effect of Inlet Geometry on NPSHr

Impeller inlet geometry is always designed for a known or assumed inlet flow condition. Impeller inlet geometry can be designed to accommodate swirling inlet flow conditions provided the details of the swirling flow are known. Circumferential or radial inlet flow asymmetry will affect the impeller performance due to the resulting variations in the impeller inlet vane incidence. Unfavorable impeller inlet vane incidence will affect both the overall impeller head generation as well as the cavitation development on the blade leading edges under low available NPSH (NPSHa). Figure 5 illustrates the impact of flow incidence angle (i) on the cavitation development and suction performance for a typical low specific speed impeller design. As seen in Figure 5, NPSH3 increases for negative blade incidence conditions (i < 0 or high flows) and decreases for positive incidence conditions (i > 0 or low flows).

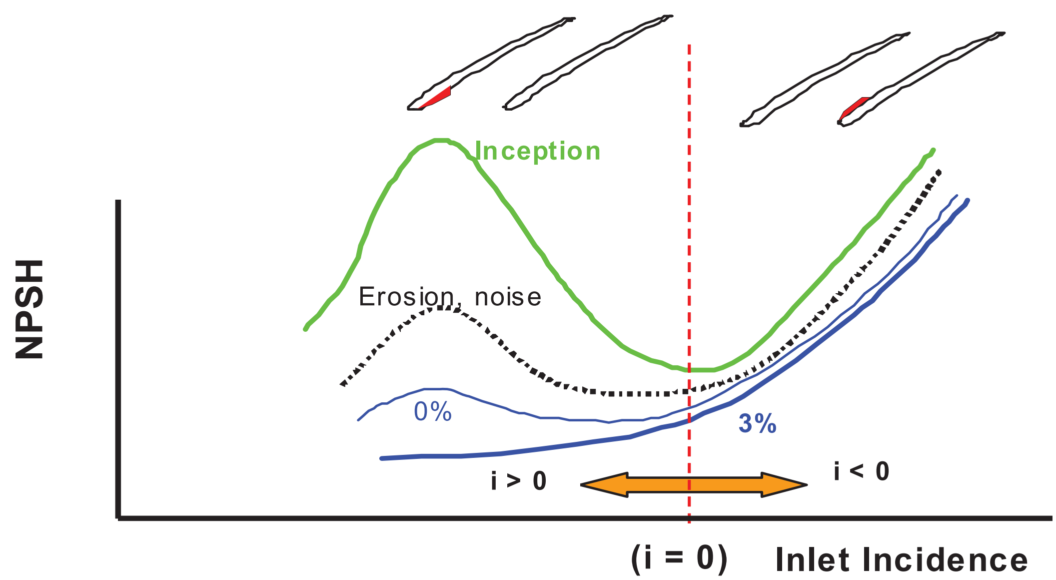

Figure 5: NPSH and Cavitation versus Inlet Incidence Angle

The flow rate in combination with upstream plant piping and pump inlet casing geometry will determine the resultant impeller eye flow distribution. To minimize the potentially detrimental effects of upstream piping induced flow disturbances, Hydraulic Institute (HI) Standard 9.6.6 [12] lists good design practices for suction inlet piping design. For instance, to reduce the impact of flow distortion caused by upstream elbows and tees, HI recommends installing a straight length of inlet pipe of at least five pipe diameters upstream of the pump suction nozzle. However, due to space constraints or other field variables, these inlet piping design recommendations are often not fully met.

2.1.1 Effects of Inlet Suction Design on NPSHr

Most public domain research work investigating the effect of pump inlet piping configuration on pump performance have focused on end suction pumps; reference Sulzer Report E12.5.1959 [1]. End suction pumps typically do not employ inlet casing designs that incorporate strong accelerating regions and flow splitters. The side inlet casing design of the CVIC pump used in the Browns Ferry RHR system will precondition the impeller inlet flow by first decelerating the flow into a plenum region before reaccelerating the flow into the eye of the impeller. Furthermore, a flow splitter (rib) is provided in the CVIC inlet casing to guide and de-swirl the flow before it enters the impeller eye. Figure 6 is a schematic representation of a cross-sectional view of a side inlet suction casing with a centerline nozzle. The figure provides a qualitative illustration of how the inlet flow splits around the axis of symmetry (pump shaft) to fill the impeller eye. On one side of the casing a pre-rotation (rotation in the direction of the impeller rotation) is induced. Pre-rotation has the effect of reducing the blade inlet incidence and shifting the low pressure region at the blade leading edge towards the blade pressure surface. This contrasts with the situation on the opposite side of the impeller eye where a counter-rotation (rotation in the opposite direction as the impeller rotation) is induced. Counter-rotation has the effect of increasing the inlet blade incidence and shifting the low pressure region at the blade leading edge towards the blade suction surface. Therefore, on each revolution of the impeller the inlet vane tips will see varying degrees of incidence as they traverse through the regions of induced pre-swirl and counter-swirl. Depending on the operating condition (flow rate) it is possible that each impeller inlet vane could experience both negative and positive inlet incidence conditions during one impeller revolution. Depending on the NPSH margin and the bubble formation characteristics of the inlet vanes, this situation could translate into periodic bubble formation on both the suction and pressure surfaces of the vanes as the impeller rotates. Upstream plant piping can induce circumferential flow asymmetry as well as swirl to the flow arriving at a pumps suction nozzle. Regardless of the pump inlet casing design, these flow variations can potentially enhance bubble formation or reduce bubble formation depending on the flow rate, the nature of the induced flow asymmetries, and also the details of the pump suction casing design. In general, it is difficult to predict the effect that any given inlet piping configuration will have on the NPSHr characteristic of a particular pump across its entire flow range. In the specific case of pumps that use side inlet casings that incorporate the above described design features it is difficult to assess a priori the impact of inlet flow disturbances on NPSHr or to use engineering judgment to determine whether the suction piping will produce a positive or a negative effect on the pump NPSHr. In general, the relative influence of upstream piping geometry on NPSH3 for end suction pumps will be greater than the corresponding influence of the same piping geometry on pumps with suction casing designs that incorporate the features described above. Therefore, the use of empirical data or engineering judgment based on experience with end suction pumps as a basis to assess the effect of inlet piping geometry on the NPSHr performance of pumps with side inlet casings is difficult at best and can lead to unexpected results.

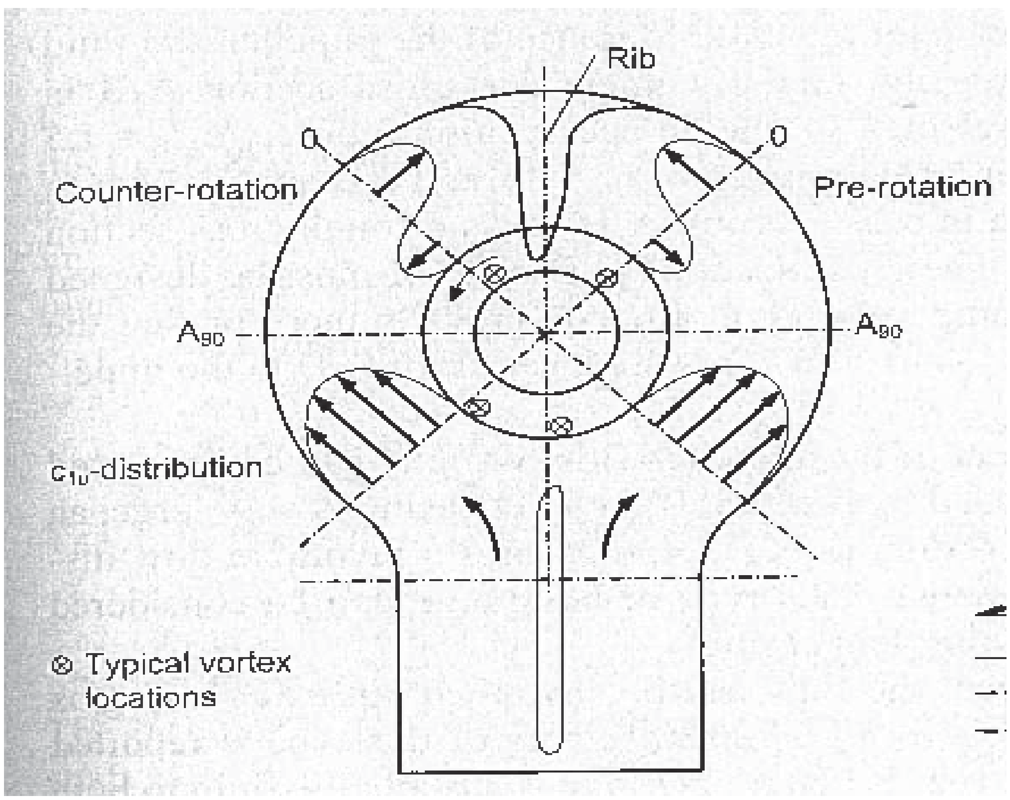

Figure 6 : Suction Inlet Flow Pattern (Gülich)

2.1.2 Browns Ferry CFD Study on Suction Piping

The baseline CFD model shown in Figure 1 was modified to include the in-situ plant inlet piping configuration that was judged to be the worst case suction piping configuration from the Browns Ferry and Peach Bottom RHR pumps (total of 20 RHR pumps). The general criteria used to assess the individual RHR pump inlet piping configurations were: 1) length of straight pipe immediately upstream of the pump suction nozzle, 2) proximity to the pump suction nozzle to piping components that would generate flow disturbances or restrictions (valves, flow branches, tees, etc.), and 3) pipe bends (elbows) upstream of the pump suction nozzle (number of elbows, plane of elbows relative to pump orientation, proximity of elbows relative to pump). The worst case plant piping selected for CFD modeling is shown as the green piping in Figure 7 and is a Browns Ferry pipe configuration. The pump CFD was run for each flow setting. Since both RHR pumps in a loop are supplied by a common supply header, the total flow rate in the common supply header is twice the pump flow rate at the three analyzed conditions ([[ ]]). The NPSH3 CFD results for the worst case plant piping are compared with the baseline CFD results as shown in Figure 8. [[

]] Although the baseline CFD shows some deviation from the test curve (Figure 4), it is reasonable to use the differences in the two CFD generated NPSH3 characteristic as an estimate of the effect of worst case suction pipe on the Browns Ferry CVIC RHR pump suction performance.

[[

]]

Figure 7 : Browns Ferry RHR Pump Suction Field Configuration

[[

]]

Figure 8 : CFD Analysis – Impact of Plant Inlet Piping on NPSH3 of Browns Ferry CVIC Pump

2.2 Effect of Fluid Temperature on NPSHr

The effect of fluid temperature on NPSHr is experimentally well-known, so CFD was not used to quantify the influence of pumpage temperature on the NPSH3 characteristic of the CVIC pump. Instead, the qualitative methods developed in the Sulzer Report E12.5.1959 [1] for the Monticello CVDS RHR pumps were used to quantify the influence of pumpage temperature on NPSH3 for the Browns Ferry CVIC pump.

NPSHr decreases as the temperature of the pumped water increases. This behavior is explained by the phenomenon of thermal dynamic suppression head (TSH). As a fluid's temperature increases, the density of the vapor increases and, therefore, the amount of energy required to produce a given volume of vapor also increases. The latent heat of vaporization required for bubble formation is provided by the surrounding liquid, which is cooled as a result, and a thermal boundary layer forms around the cavitation bubble. With increasing fluid temperature the energy required to produce a given volume of vapor increases which amplifies the thermal boundary layer. The thermal boundary layer will act as an insulator restricting energy transfer from the surrounding liquid and limiting bubble growth.

The magnitude of the TSH effect is fluid and temperature dependant. These dependencies were documented in some detail in the Sulzer Report E12.5.1959 [1] and are not repeated here other than to say that the magnitude of the thermal suppression effect for low temperature water is quite small and can be ignored. At water temperatures approaching [[ ]], the improvement in NPSH3 becomes finite [[ ]] and consideration should be given to including the benefit in the pump NPSH analysis to offset negative uncertainties or to show margin. In the next paragraph, examples are provided that show the magnitude of the temperature effect.

During Design Base Accident Loss-of-Coolant (DBA-LOCA) the RHR pumps may be postulated to operate with suppression pool temperatures in the range of [[ ]]. Using the TSH charts obtained from the public literature and summarized in Sulzer Report E12.5.1959 [1], reductions in NPSH3 of approximately [[

]] are calculated. For the long-term LOCA condition at flows of [[ ]], the relative effect of a [[ ]] decrease in NPSH3 is significant. For example, at [[

]] improvement in NPSH3. At [[

]] improvement.

2.3 Effect of Dissolved Air on NPSHr

Project plans to use CFD to characterize the effects of dissolved gas on NPSH3 were terminated to focus CFD resources on evaluating effects of pump inlet pipe geometry and pump wear ring clearance on NPSH3. However, the qualitative methods developed in the Sulzer Report E12.5.1959 [1] for the Monticello CVDS RHR pumps can be used to provide an estimate of the influence of dissolved gas on NPSH3 for the CVIC pump. Additionally, a literature survey on the effects of dissolved gas on NPSH3 was provided in Sulzer Report E12.5.1959 [1].

The solubility of air in water depends on air pressure and water temperature. Solubility is a weak function of pressure (increases with increasing pressure) and decreases strongly with increasing water temperature up to approximately 212 ºF. Since BWR containments are maintained near atmospheric pressure, the amount of dissolved gas in the suppression pool water is governed by the gas saturation solubility at atmospheric pressure and the suppression pool water temperature.

The effect of inlet gas void fraction (GVF) on pump discharge performance has been widely studied; for example Florjancic [2]. However, the effect of inlet GVF on NPSHr has not been well documented in the public literature. Budris and Mayleben [3] published some test results which described the influence of GVF on pump inlet dynamic pressure pulsations in the presence of cavitation. Research shows that small amounts of gas (approximately 0.5 - 2% by volume fraction) do not cause any significant impact on a pump's discharge performance. It has also been demonstrated that the introduction of small amounts of air can actually reduce pump noise, vibration, and cavitation damage by absorbing some of the implosion energy of the cavitation bubbles. [[

]]

2.3.1 Approach for Estimating Impact of Gas Void Fraction on NPSH3

Based on the gas blockage model described above, a one-dimensional flow analysis was conducted to predict the degradation of pump discharge head and increase in NPSH3 resulting from the presence of dissolved gas in the Browns Ferry CVIC pump. [[

]]

[[

]]

Figure 9: Browns Ferry RHR Pump - Effect of Dissolved Gas (2% GVF) on NPSH3

Figure 9 provides an example of this method for estimating the change in NPSH3 [[

]]

2.3.2 Dissolved Gas in Suppression Pool Water

To assess the effective impact of dissolved gas (inlet GVF) on pump performance, the interaction of the degraded pump head versus flow characteristic with the system characteristic must be considered. This interaction is illustrated in Figure 10 where the Browns Ferry RHR system characteristic (orange curve) is superimposed on the two pumps in parallel CVIC pump characteristics: 1) the non-degraded flow characteristic (red curve) and 2) the degraded characteristic (blue curve). [[

]]

[[

]]

Figure 10: Browns Ferry RHR – System Interaction with Two Pumps in Parallel Characteristic

According to the BWROG committee, the normal suppression pool water temperature is in the range of [[ ]] and the wetwell air space above the pool is composed of [[ ]] at near atmospheric pressure. Since the wetwell air space and suppression pool water are in contact for long periods of time, the dissolved gas concentration in the pool water is assumed to be at equilibrium with the wetwell air space. Based on the assumption of gas saturated suppression pool water a gas solubility calculation was made using Henry's gas law. If all the dissolved gas in the suppression pool was to instantly come out of solution at atmospheric pressure the following GVF's would result: [[ ]]. Per the BWROG committee, using [[ ]] as the initial suppression pool temperature in LOCA analyses versus a lower initial pool temperature [[ ]] is more limiting with regard to NPSH. This is because with a starting temperature of [[ ]], at the end of short-term LOCA analysis [[ ]] the pool temperature is [[ ]] The potential negative effects of a higher initial dissolved gas concentration at the lower temperature [[ ]] are compensated for by the gain in NPSHa at [[ ]]. Therefore, with regard to dissolved gas effects on NPSH3, use of [[ ]] as the initial pool temperature is conservative.

Evolution of dissolved gas from a liquid is a diffusion process, which takes time, and only a fraction of dissolved gas would evolve out of solution due to the short residency time as a slug of fluid transits through the low pressure inlet region of the impeller in a single pass through the pump. Also, the suppression pool normal water level is about [[ ]] above the RHR pump suction elevation and the static pressure at the pump suction will be greater than atmospheric during most time frames in LOCA calculations even when accounting for pressure loss across the system suction strainers and the suction pipe friction losses. This serves to keep gas in solution.

Appendix A3 of Reference 4 provides an approach for determining GVF based on the differences in the gas solubility between two locations in a fluid system. In this approach, Henry's Law is used to quantify the solubility of the gas mixture in the suppression pool (reservoir temperature and pressure) and at the local pressure at the impeller eye. The amount of gas available to come out of solution at the impeller eye is calculated as the difference in gas solubility between the reservoir conditions and the impeller eye conditions. The pressure at the RHR pump inlet was provided by BWROG for selected flow rates and is based on the water elevation head in the suppression pool reduced by pressure loss across the strainers and the suction pipe friction head loss. The pressure at the impeller eye was calculated from the difference between the pump inlet pressure and the pressure loss in the pump inlet casing less the change in fluid velocity head between the pump suction nozzle and the impeller eye. Table 3 provides a summary of the pump inlet pressures provided by BWROG, the pump inlet casing pressure loss, the change in velocity head between the inlet nozzle and the impeller inlet, and the resultant calculated impeller inlet static pressure for RHR flows of [[ ]].

During the short-term LOCA phase, the static pressure at RHR pump inlet may decrease below atmospheric pressure depending on the system modeling assumptions at high RHR flows with strainer plugging (i.e., the net pressure drop across the strainers and pump suction piping is greater than elevation head between the suppression pool and the pump inlet). The minimum static pressure at the RHR pump inlet nozzle [[ ]] in Table 3 represents the Browns Ferry short-term LOCA phase for RHR flow to the broken recirculation loop at [[ ]] RHR flow with fully debris loaded strainers at [[ ]] and no containment accident pressure (CAP).

	Pump Flow Rate (gpm)		
	[[		
Pump Inlet Pressure (psig)			
Head Loss in Inlet Casing (ft)			
Increase in Velocity Head from Suction Nozzle to Impeller Eye (ft)			
Impeller Inlet Pressure (psig)			]]

Table 3: Summary of Pump Inlet Pressures and Losses Through Inlet Casing

The estimated GVFs and the associated changes in RHR NPSH3 based on the difference between the gas solubility in the suppression pool and at the pump impeller inlet have been determined and are tabulated in Table 4 for various RHR flows and fluid temperatures. The values in Table 4 were calculated based on the following assumptions: [[

]]

[[

]]

Table 4: GVF at Pump and Impeller Inlet Using Calculation Method from Reference 4 and Respective Pressures from Table 3

As shown in Table 4, for the short-term LOCA at high RHR flow rates [[ ]], the calculated GVF based on local pump pressure is small [[ ]]. The largest impact is seen at 155 °F, where an increase of .5 ft is calculated for NPSH3, which is likewise small. The inclusion of CAP would further increase the static pressure at the pump impeller if included. [[

]]

[[

]]

Figure 11: Browns Ferry RHR – System Interaction with Two Pumps in Parallel Characteristic

Table 3 shows that for the [[ ]] flow rate cases, the impeller inlet pressures are always greater than atmospheric pressure. Consequently, no dissolved gas will come out of solution. This is reflected in Table 4 as a zero GVF% for all water temperatures. Table 4 also provides the estimated GVF using the pressure at the pump suction nozzle for the high flow case [[ ]] to provide a comparison point with industry documents that use GVF at the pump suction as a reference condition.

After the short-term LOCA phase [[ ]] the RHR flow is reduced by the operator, which markedly increases the pump suction pressure (see Table 3) and keeps dissolved gas in solution as shown in Table 4 for [[ ]] cases. The rate of pool temperature increase during the long-term LOCA phase is slow and a maximum pool temperature is not reached until several hours into the event. During this time period the dissolved gas content would continually decrease due to increased water temperature (reduces gas solubility) and the degassing effects of continuously recirculating the pool water inventory through the RHR and Core Spray pumps. For long-term LOCA, the combined affects of decreasing gas solubility due to higher pool temperatures and the continuous degassing effects of pump operation will result in reducing dissolved gas content to a very low value prior to encountering peak pool temperatures where NPSHa issues may be encountered. Additionally, as discussed in Section 2.2, at high water temperatures the TSH effect provides an improvement in NPSH3, which further offsets any dissolved gas effects. Accordingly, NPSH3 uncertainty due to dissolved gas is limited to the short-term phase of the DBA-LOCA event [[ ]]

A further consideration relevant for this discussion on effects of dissolved gas on BFN RHR pump performance is the recognition that the original factory pump test results, which form the reference basis for comparison in this NPSHr discussion, were measured using water that was not completely deaerated. Therefore, the reference NPSHr characteristic will already include some effects of dissolved gas coming out of solution during the factory NPSHr characterization test.

2.4 Effect of Wear Ring Clearance on NPSHr

Wear rings provide a restricted clearance feature between rotating and stationary components inside a centrifugal pump. During operation, a small percentage of the impeller outlet flow leaks through the wear rings back into the impeller inlet as shown in Figure 12. The amount of leakage depends on the wear ring clearance and the pressure difference across the wear ring. Increasing wear ring clearance increases the leakage flow and also the flow through the impeller if a constant pump discharge flow rate is maintained. The net effect is a reduction in discharge head and an increase in NPSH3 at the same effective pump discharge flow rate. In this section of the report, an approach for estimating the impact of wear ring clearance on pump NPSHr is provided.

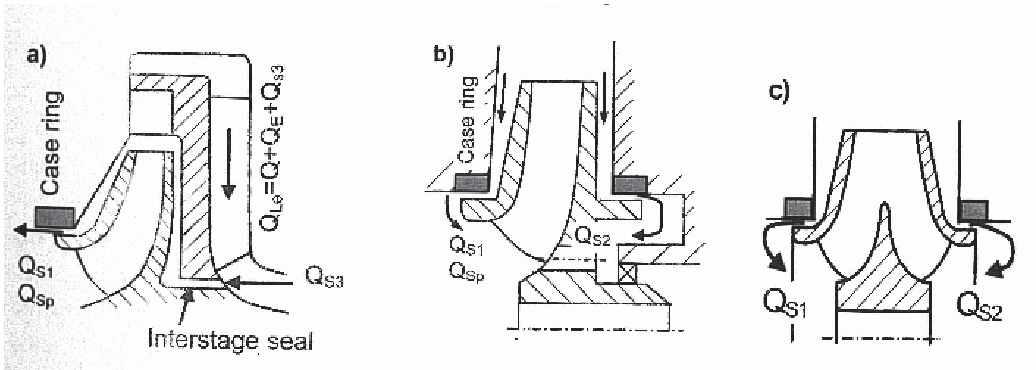

Figure 12: Wear Ring Leakage (Gulich)

2.4.1 Browns Ferry CFD Study on Wear Ring Clearances

The nominal (new condition) wear ring clearances from the baseline CFD model for the Browns Ferry CVIC pump were increased to two times (2x) their nominal value. The increased wear ring clearance CFD model was run at three flow rates, [[ ]] using the same straight inlet pipe geometry as the baseline CFD model. NPSH3 CFD results from the 2x wear ring clearance case and the baseline CFD case are shown in Figure 13. [[

]]

[[

]]

Figure 13: Impact of Wear Ring Clearance on NPSHr of Browns Ferry RHR Pump Using CFD

2.4.2 Approach for Estimating Impact of Wear Ring Clearance on NPSHr

The contribution to the NPSHr uncertainty due to increase in wear ring clearance depends on the wear ring clearance at the beginning of the DBA-LOCA event and any additional wear accrued during the mission time. Based on a BWROG survey of member plants, operating hours for RHR pumps is typically much less than [[ ]]. This amount of ordinary use is small compared with the expected pump wear ring life, which depending on pumpage and wear ring material may be equivalent to several years of continuous pump operation. The infrequent pump operation combined with actual plant-specific operating experience (pump maintenance frequency) and periodic pump surveillance testing, which monitors and trends pump performance, collectively provide reasonable assurance that the pump wear ring clearance prior to the LOCA will be within required tolerances. The additional pump duty accrued during a [[ ]] mission time for the analyzed event is [[ ]], which again is small compared to the expected life of impeller wear rings. Should examination of plant data conclude that wear ring wear is small, then the wear ring contribution to the overall NPSHr uncertainty would also be small and, thus, may be omitted from the NPSHr uncertainty assessment. However, where examination of plant data indicates that the wear ring wear is not small enough to be neglected, it is prudent to determine what the resulting effect would be on NPSHr uncertainty using the CFD results shown in Figure 13. A normal operating CVIC pump (configured and operating within the manufacturer's specifications and guidelines) is not expected to experience an appreciable increase in wear ring clearance during the [[ ]] of operation after a LOCA event. Therefore, a conservative estimate of the maximum effect of increased wear ring clearance on NPSH3 uncertainty can be obtained from the CFD results provided in Figure 13.

[[

]]

[[

]]

Figure 14: Browns Ferry RHR Pump - Effect of 2x Wear Ring Clearance on NPSH3

The above system interaction discussion is for the short-term LOCA condition, nominal [[ ]] system flow. For the long-term LOCA phase, the system is throttled to move the operating point to a lower flow characteristic. In this analysis, the evaluated flows are [[ ]]. Due to the shape of the NPSH3 curve at low flows (Figure 14) as the pump operating flow rate is reduced below approximately [[ ]] the NPSH3 for the worn condition improves (is lower than) the NPSH3 for the nominal or new wear ring condition. To quantitatively assess the NPSH3 impact at the long-term LOCA flow rates the new system curve can be superimposed on the 2 pump in parallel pump characteristics and a similar exercise as is illustrated in Figure 14 conducted.

3.0 Combined NPSHr Uncertainties

The primary objective of this report is to establish a methodology to quantify both the individual and combined uncertainty contributions of various system and pump related variables on RHR pump NPSHr. The effects of the following pump related variables were examined: 1) plant piping geometry 2) fluid temperature 3) dissolved gas and 4) wear ring clearance.

The contribution to the NPSHr uncertainty due to in-situ plant piping geometry was evaluated using CFD. Relative to the baseline (straight inlet pipe) CFD, an increase in NPSH3 of [[ ]] was predicted for the worst case in-situ plant inlet pipe configuration as selected from the combined Browns Ferry and Peach Bottom RHR pump population. At the lowest evaluated RHR flow of [[ ]] the NPSH3 remained unchanged between the baseline and the worst case plant piping configuration for the selected inlet pipe configuration.

The NPSHr uncertainty contribution due to pumpage temperature (TSH effect) is insignificant at low temperatures [[ ]] and increases to approximately [[ ]] at higher suppression pool temperatures [[ ]] In the case of the Browns Ferry CVIC RHR pumps this translates to an improvement in NPSH3 uncertainty of [[ ]], respectively.

The NPSH3 uncertainty contribution due to dissolved gas in the pumpage (water) is dependent on both the fluid temperature and on the pump relative operating point. At the end of the short-term LOCA phase [[ ]] the estimated NPSH3 increase from release of dissolved gas [[ ]]. For the long-term LOCA, at the [[ ]] flow rate cases, the impeller inlet pressures are always greater than atmospheric pressure. Consequently, no dissolved gas will come out of solution. Table 4 shows the GVFs at other water temperatures. The analysis demonstrates that NPSH3 uncertainty is a factor only in short-term phase of the DBA-LOCA event.

Regarding wear ring clearance effects, where examination of plant data concludes that pump wear ring wear is small, then the wear ring contribution to the overall NPSHr uncertainty will also be small and it may be excluded from the NPSH uncertainty assessment. However, should examination of plant data conclude that pump wear ring wear is not small enough to be excluded from the overall NPSHr uncertainty assessment, then the wear ring contribution can be included in the overall NPSHr uncertainty using the methodology outlined for the Monticello RHR pump in Sulzer Report E12.5.1959 [1].

Using a maximum permissible wear ring clearance of 2 times design clearance as the fully worn condition for the Browns Ferry CVIC RHR pumps at the design flow of [[ ]], the fixed bias or average NPSHr uncertainty ($\Delta_{wear\_ring\_fixed}$) due to wear ring clearance increase would be approximately 50% of the total uncertainty at 2 times clearance or [[ ]] The random uncertainty ($\Delta_{wear\_ring\_random}$) due to wear ring clearance would be [[ ]] Thus, the NPSHr uncertainty due to wear ring clearance can be expressed as:

[[ ]]

Reference [5] provided an equation for adjusting NPSHr for pump speed variations. The Reference [5] example was for speed variations of [[ ]]. Pump operating speed variance [5] and test measurement uncertainty [6] contribute approximately [[ ]] respectively, to the NPSHr uncertainty for the CVIC RHR pumps at the rated flow condition of [[ ]]. The uncertainty contribution from these two factors are classified as random uncertainties so their combined effect (when wear ring wear is small and is not included in the overall NPSH uncertainty) can be quantified by using the Square Root of the Sum of Squares (SRSS) method. A generic representation of the combined random uncertainty due to pump operating speed variance and test bed measurement uncertainty is:

[[ ]]

The uncertainty contribution from these two factors are classified as random uncertainties so their combined effect along with the random uncertainty contribution from the wear rings can be quantified by using the SRSS method. If a 2 times increase in wear ring clearance is used as the maximum clearance criterion for the Browns Ferry RHR pumps, then the combined random uncertainty contributions due to pump operating speed variance, test bed measurement uncertainty, and wear ring wear is:

[[ ]]

The combined total generic NPSHr uncertainty at high flows and high suppression pool temperatures [[ ]] when the wear ring contributions are negligibly small, is computed as the sum of the fixed bias uncertainties plus or minus the total random uncertainty and is given by,

[[ ]]

Thus, at high suppression pool temperatures when wear ring wear is minimal and is excluded from the total NPSH3 uncertainty, the total NPSH3 uncertainty is likely to vary from approximately [[ ]]

However, should it be necessary to include the effects of wear ring wear in the total NPSH3 uncertainty at high flows [[ ]] and high suppression pool temperatures [[ ]], then a generic representation for the combined NPSHr uncertainty is computed as the sum of the fixed bias uncertainties plus or minus the total random uncertainty and is given by:

[[ ]]

In the specific context of the Browns Ferry RHR pumps where 2 times wear ring clearance is used for the maximum allowable wear ring wear criterion, the total NPSHr uncertainty can be expressed as:

[[ ]]

In the specific example of the Browns Ferry RHR pumps where the NPSH uncertainty due to speed variation is taken as [[ ]] and the maximum wear ring clearance criterion is 2 times nominal (design) clearance, then the combined NPSH uncertainty at high flows [[ ]] and high suppression pool temperatures [[ ]] is likely to vary from approximately [[ ]] on the high side to [[ ]] on the low side. The effects of both dissolved gas (inlet GVF) and increased wear ring clearance on NPSH will depend on the interaction of the resultant degraded pump curve and the system curve. The effective change in NPSH due to these two factors will, in effect, be less than if their effects are taken at a constant flow rate. Therefore, the above estimate should provide a conservative estimate of the NPSH uncertainty.

Appendix A provides a summary table of combined NPSH3 uncertainty estimates for the Browns Ferry RHR pumps at three flow rates, [[ ]] at various inlet temperatures and inlet GVF conditions. The uncertainty values presented in Appendix A were calculated using the NPSH3 uncertainty data and calculation methodologies developed in this report.

4.0 Conclusions

This report combined CFD results and analytical methods to determine the impact of various pump parameters on the overall NPSHr uncertainty of the Browns Ferry RHR pumps. The NPSH3 uncertainties computed in this report using both CFD and analytical methods are a conservative estimate of the combined effects from several different variables that can affect the pump NPSH3. The effects of pump suction piping geometry, fluid temperature, dissolved gas, wear ring clearance, pump operating speed variance, and test measurement uncertainty have all been, to the extent reasonably practical, quantified and combined to express a total NPSH3 uncertainty for a Sulzer CVIC pump used in the RHR system at the Browns Ferry and Peach Bottom Nuclear Generating Plants.

Although the analytical methods discussed in this report can be applied to other pump/plant applications it is important that a thorough analysis of the pump design and system specifics be conducted to determine an appropriate NPSHr uncertainty value for each parameter. For example, if the temperature of the suppression pool is high (above [[ ]]), then the contribution of dissolved gases to uncertainty is low. If a plant has a suction piping design which causes few distortions in the inlet flow, then the plant piping NPSH uncertainty will likely be lower than that computed for the BFN pump in this report. Similarly, if the pump's wear ring clearance is known to be small (at or near manufacturers design value), then using two times wear ring clearance for the NPSH uncertainty analysis may be too conservative.

This report uses a statistical method for combining NPSH uncertainty values for obtaining an overall NPSH3 uncertainty for the Browns Ferry CVIC RHR pump. This method utilizes the general approach adopted for combining random and systematic uncertainties and provides a conservative overall NPSH3 uncertainty for the pump. The results (Appendix A) provide reasonable assurance that the NPSHr uncertainty is less than 21% for the CVIC pump at the pump flow rates and temperatures that would be expected during LOCA. Noteworthy among these uncertainty contributors is allowance for a pump speed variation of up to [[

]]

Generic applicability and limitations:

Generic applicability, cautions, and limitations on the use of specific values provided within this and related contributing task reports include the following:

- Speed uncertainty methodology [5] can be generically applied to directly coupled motor driven pumps
- Test instrumentation uncertainty methodology [6] can be generically applied to most any pump while the specific uncertainty values cited in the report are applicable to Sulzer pumps with similar operating parameters (head, flow, and RPM) as the Browns Ferry/Peach Bottom RHR pumps
- The magnitude of the temperature effects can be generically applied to any BWR ECCS pumps taking suction from the suppression pool with peak pool temperatures in the range of 60 °F to 210 °F
- Dissolved gas uncertainty should be limited to pumps of similar hydraulic design as the Sulzer CVIC pumps used for RHR service at Browns Ferry operating at a similar relative point on their pump curves and taking suction from a suppression pool with peak pool temperatures in the range of 60 °F to 210 °F
- The plant piping uncertainty values determined from CFD for the specific inlet pipe geometry investigated in this report should not be applied generically.
- NPSH3 uncertainty values calculated in this report due to suction piping geometry are considered bounding for the geometry identified, but a detailed review of site specific geometry is required to confirm applicability.
- Wear ring uncertainty effects should be evaluated on a plant specific basis. A methodology was developed for determining the magnitude of the NPSH3 uncertainty contribution due to increased wear ring clearance. A procedure, based on plant specific maximum wear ring clearance criteria and pump performance monitoring data, was developed to calculate the wear ring NPSH3 uncertainty contribution. Finally, a representative example calculation, using the Browns Ferry RHR pumps maximum wear ring clearance criteria, was presented to illustrate the uncertainty contribution due to wear ring clearance effects.

The results reported are representative for the specific evaluated application, the Browns Ferry CVIC RHR pumps, and provide assurance that use of a generic 21% NPSH3 uncertainty for similar pumps in similar service conditions is a reasonable and bounding value.

Bibliography

1. Dan Baun & Ankur Kalra, "Task 1 - CFD Report and Combined NPSHr Uncertainty for Monticello RHR CVDS Pump", Sulzer Report E12.5.1959, June 18, 2012.
2. D. Florjancic, "Influence of Gas and Air Admission on the Behavior of Single and Multistage Pumps", Sulzer Research Number 1970.
3. Allan R. Budris, Philip A. Mayleben, "Effects of Entrained Air, NPSH Margin, And Suction Piping on Cavitation in Centrifugal Pumps",1998.
4. Centrifugal Pumps, Johann Gülich, 2nd Edition, Appendix A, Figure A3.2.
5. Ankur Kalra, "Task 2 – Equation for Pump Speed Correction Sulzer Pumps (US) Inc. Browns Ferry & Peach Bottom – RHR Pumps", Sulzer Report E12.5.1940, Nov 4, 2012.
6. Ankur Kalra, "Task 6 – NPSHr Test Instrumentation Accuracy Affect on the Published Results, Sulzer Pumps (US) Inc. Browns Ferry & Peach Bottom – 18x24x28 CVIC RHR Pump", Sulzer Report E12.5.1950, April 30, 2012.
7. Centrifugal Pumps, Johann Gülich, 2nd Edition, Chapter 6.
8. Pumps and Blowers Two-Phase Flow, Stepanoff.
9. Miriam Roth Kliem, "Experimentelle und Numerische Untersuchung zum Einfluss von Einbaubedingungen auf das Betriebs – und Kavitationsverhalten von Kreiselpumpen", 2006.
10. Bujnes, J. H., Op De Woerd, J.,1984, "Erosion Free Operation of Cavitating Pump", Proceedings of the 2nd European Congress on Fluid Machinery for the Oil, Petrochemical and Related Industries, The Hague, The Netherlands, IMechE Conference Publications 1984-2, Paper C28.
11. Terry Henshaw, P. E, "Effect of Internal Clearances on NPSHR", Pumps and Systems, July 2009.
12. ANSI/HI 9.6.6-2009, America National Standard for Rotodynamic Pumps for Pump Piping, New Jersey.
13. Bruno Schiavello, " Visual Study of Cavitation – An Engineering Tool to Improve Pump Reliability", Proceedings of EPRI 1st International Conference on Improve Coal-Fired Power Plants, Palo Alto, California.
14. B. Le Fur (Mrs.), J. F. David, D.Le'cot, "Influence de l'air occlus et dissous dans l'eau sur le comportement des pompes en cavitation", CETIM, Nantes
15. ANSI/HI 1.3-2009, Rotodynamic (Centrifugal) Pump Applications

5.0 Appendix A: Browns Ferry CVIC NPSH3 Uncertainty Summary Table

CVIC Uncertainty (Percentage) *Note 5

[[					
				]]

[[

]]